Progress on the reevaluation and validation of the n+^{233}U neutron cross sections

Marco T. Pigni[a,*], Roberto Capote[b], Andrej Trkov[c]

[a] *Oak Ridge National Laboratory, Oak Ridge, Tennessee 37831, USA*
[b] *NAPC–Nuclear Data Section, International Atomic Energy Agency, Vienna, Austria*
[c] *Jožef Stefan Institute, Jamova cesta 39, 1000 Ljubljana, Slovenia*

Abstract

^{233}U resonance parameters of the ENDF/B-VIII.0 nuclear data library were adopted from previous ENDF/B-VII.1 evaluation using the external levels to update the thermal values. Adoption of IAEA 2017 thermal standards ($\sigma_f = 533.0 \pm 2.2$ b, $\sigma_c = 44.9 \pm 0.9$ b, and $\overline{\nu}_{tot} = 2.487 \pm 0.011$) and of the IAEA recommended thermal-neutron induced prompt fission neutron spectrum (PFNS) with average PFNS energy of 2.030 ± 0.013 MeV require a re-evaluation of ^{233}U neutron cross sections in the resolved resonance region. A newly produced evaluation is being tested on carefully selected benchmarks from the Handbook of International Criticality Safety Benchmark Experiments (ICSBEP) which are highly sensitive to ^{233}U data. An important goal of this work was to eliminate the strong negative gradient of the calculated effective multiplication factors k_{eff} with respect to the epithermal fission fraction observed in ENDF/B-VIII.0 validation for those assemblies. A significant improvement in integral performance of critical ^{233}U solutions is observed for the newly proposed evaluation. Further work addressing the fast neutron region is needed.

*Corresponding author
Email addresses: pignimt@ornl.gov (Marco T. Pigni), R.CapoteNoy@iaea.org (Roberto Capote), Andrej.Trkov@ijs.si (Andrej Trkov)

This manuscript has been authored by UT-Battelle, LLC, under contract DE-AC05-00OR22725 with the US Department of Energy (DOE). The US government retains and the publisher, by accepting the article for publication, acknowledges that the US government retains a nonexclusive, paid-up, irrevocable, worldwide license to publish or reproduce the published form of this manuscript, or allow others to do so, for US government purposes. DOE will provide public access to these results of federally sponsored research in accordance with the DOE Public Access Plan (http://energy.gov/downloads/doe-public-access-plan).

Keywords: *R*-matrix, ^{233}U, fissile nuclide, validation, nuclear data, evaluated data.

1. Introduction

The neutron fission and capture cross sections of ^{233}U are of paramount importance to criticality safety, shipping communities, and the development of different reactor designs, including breeder reactors. Particularly within the Nuclear Criticality Safety Program, the measurement and related evaluation of the neutron resonance parameters of ^{233}U have been identified as priorities for the support of criticality safety analyses of the fuel drain and fuel flush tank of the Oak Ridge National Laboratory (ORNL) Molten Salt Reactor Experiment.

Additionally, the ^{233}U is the fissile nucleus of the thorium-based nuclear fuel cycle (often called Th/U fuel cycle). The Th/U fuel cycle offers many advantages for future energy production that have been discussed by the International Atomic Energy Agency [1, 2] including proliferation resistance, much smaller build-up of long-lived higher actinides which are the main source of long-term residual radioactivity in nuclear waste, and the fact that world reserves of thorium are much larger than uranium reserves. The above advantages have resulted in an increasing worldwide interest in innovative fuel cycle concepts based on thorium like some Molten Salt Reactors.

In light of the strong negative gradient as a function of the epithermal fission fraction (FEPIT) observed in both ENDF/B-VII.1 and ENDF/B-VIII.0 nuclear data libraries [3, 4], the aim of the present work is to check the adequacy of the integral measurements reported in the International Criticality Safety Benchmark Evaluation Project (ICSBEP) Handbook [5], as well as to verify the trend and whether it is caused by ^{233}U or some other operational materials present in the benchmarks. At the same time, the need of a reevaluation of the ^{233}U resonance parameters is motivated by updated thermal neutron constants [6] as well as by recent fission cross-section measurements [7] reporting an underes-

timation of up to 10% in the evaluated fission cross sections of the recently released ENDF/B-VIII.0 nuclear data library. In fact, although the previous R-matrix analysis performed by Luiz Leal [8] was built on precise ^{233}U(n,f) and ^{233}U(n,tot) cross section measurements [9, 10] performed at the Oak Ridge Electron Linear Accelerator (ORELA) (1997–2000), only the shapes of ORELA fission cross sections were used to determine their magnitude.

Also of interest is the expectation that high-leakage fissile solutions are very sensitive to prompt fission neutron spectra (PFNS) average energy; and a lower value of the PFNS average energy increases criticality significantly, as demonstrated in Ref. [11].

The average PFNS energy of 2.030 ± 0.013 MeV used in the new evaluation was derived using a non-model fit of available data from the work on standards at the International Atomic Energy Agency (IAEA) [6, 12]. This derived PFNS was significantly softer than previously used values of 2.074 MeV in both ENDF/B-VII.1 and ENDF/B-VIII.0 nuclear data libraries [3, 4].

Because of the important interplay between the reaction cross sections and the PFNS in benchmark calculations, there was a clear need to update the resonance evaluation once the PFNS was updated. The newly adopted PFNS was composed in the high-incident-energy range by the PFNS evaluated by M. Rising et al. [13] within the coordinated research project on the PFNS of actinides [14] and contributed by Patrick Talou from the Los Alamos National Laboratory [12].

The importance of the n+^{233}U data for nuclear applications is justified by both experimental and validation parallel activities performed in Europe. Among these, there is the recent experimental work performed at the n_TOF facility to measure the ^{233}U α-ratio [15] as well as the extensive work to validate actinide nuclear data based on reactivity experiments [16].

2. Initial Benchmark Analysis

To check the possible bias introduced by the use of operational materials such as beryllium or polyethylene as reflectors in the benchmarked ^{233}U solutions,

the first test was performed on an evaluated data file updated only with the PFNS component and based on the reaction cross sections reconstructed from the resonance parameters reported in the ENDF/B-VIII.0 library.

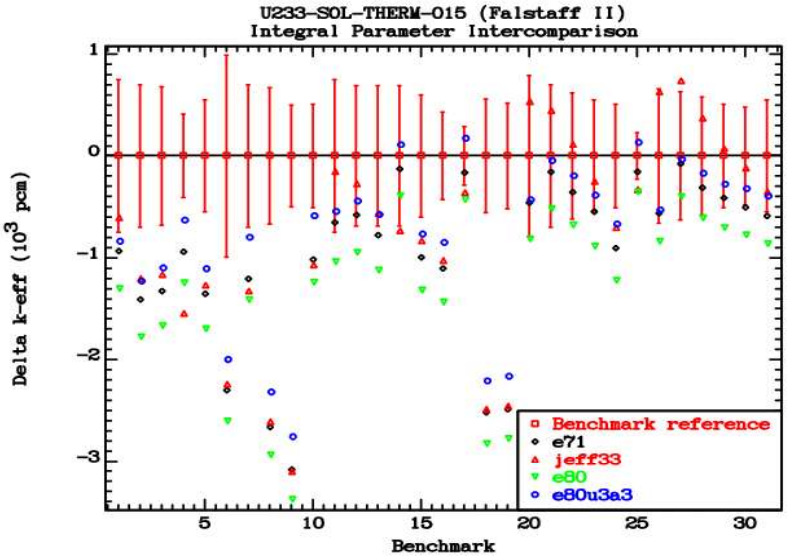

Figure 1: Comparison between measured and predicted reactivity as a function of the case number for the 31 cases of the U233-SOL-THERM-015 benchmark. The calculated reactivity refers to ENDF/B-VII.1 ("e71"), JEFF-3.3 ("jeff33"), ENDF/B-VIII.0 ("e80"), and current work ("**e80u3a3**").

Calculated reactivities of the ^{233}U solution benchmarks are widely scattered, which makes it difficult to identify biases and trends in the results. For this reason, initial analysis was done on a series of cases denoted in the ICSBEP Handbook as U233-SOL-THERM-015, abbreviated UST015 for short. The benchmark solutions were part of the Falstaff program carried out at the Lawrence Livermore National Laboratory in 1950s with beryllium and polyethylene–reflected uranyl-fluoride solutions in spherical vessels of different sizes. The set consisted of 31 cases with nitrate solutions of different concentrations and with different sphere diameters and reflector thicknesses. The predicted reactivity as a function of the FEPIT (sometimes referred to as the above-thermal fission fraction), calculated using the provided benchmark computational models

for MCNP, is shown in Fig. 1 using evaluated data from ENDF/B-VII.1 [3], ENDF/B-VIII.0 [4], JEFF-3.3 [17], and the current work (labeled "**e80u3a3**"). The results compare with the benchmark measured values similarly to the trend reported in the ENDF/B-VIII.0 nuclear data library, with the notable exception of a large positive shift in reactivity of about 500 pcm for the updated library. This shift is consistent with the fact that the newly evaluated data feature a softer neutron spectrum than seen in previous evaluations, therefore increasing the criticality for small spherical solution assemblies with relatively large leakage-neutron fraction.

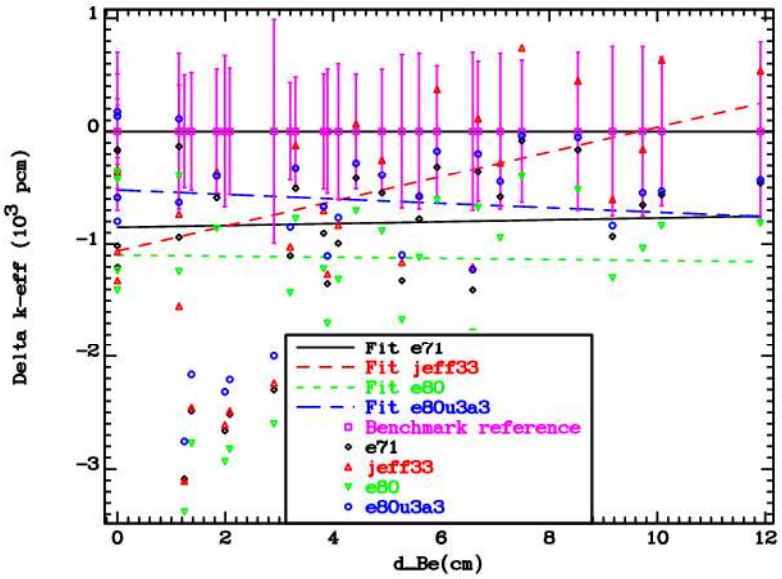

Figure 2: Comparison between measured and predicted reactivity of UST015 cases as a function of the beryllium reflector thickness d_{Be}.

To study the impact of reflectors on UST015 criticality, the same data are plotted as a function of beryllium reflector thickness in Fig. 2. Benchmark solutions containing only polyethylene reflectors do not show any significant gradient for any of the evaluated libraries, and the calculated reactivities are practically within the uncertainty band for the updated ^{233}U evaluation. Benchmark solutions containing thin beryllium reflectors (below 3 cm thickness) without

polyethylene seem to strongly underpredict reactivity. Most of the remaining cases agree fairly well with the reference benchmark values for the **e80u3a3** evaluated file.

As highlighted in Table 1, the underprediction of reactivity seems to be strongly emphasized in assemblies featuring only beryllium reflectors thinner than 3 cm, e.g., cases 6, 8, 9, 18, and 19 (marked with *). Polyethylene reflectors do not exhibit a similar trend (e.g., cases 7, 10, 17, 25); neither is such a trend observed in cases that have an additional polyethylene layer on the outside of the beryllium reflector (e.g., cases 4 and 14). Since only the cases with a thin beryllium reflectors deviate from the general trends, we assumed there could be unidentified problems with measurements or benchmark specifications, so we excluded them from the subsequent analysis. After excluding the cases with

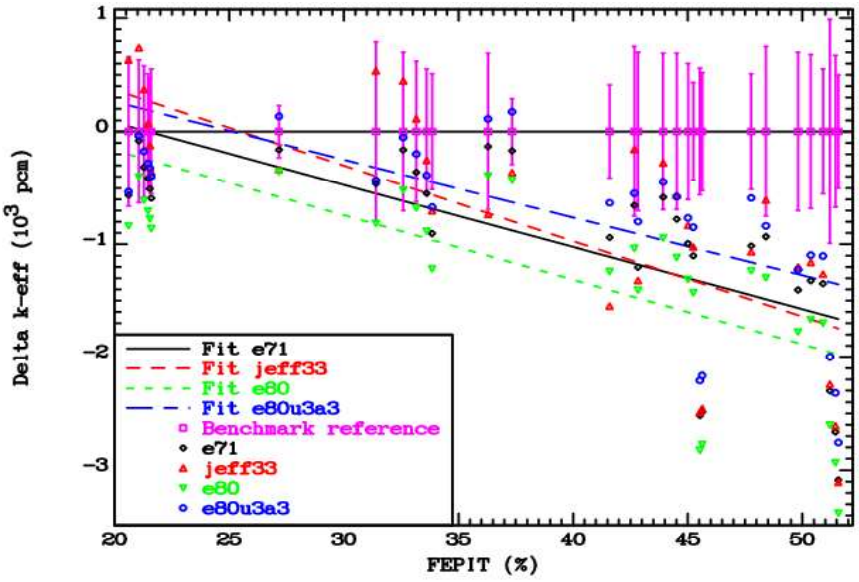

Figure 3: Differences in predicted reactivity from the reference benchmark value as a function of the epithermal fission fraction, FEPIT, without the thin beryllium outliers.

thin beryllium reflectors the problem in the underestimation of reactivity is still evident, as shown in Fig. 3. The gradient in reactivity as a function of FEPIT is marked by a large decrease in reactivity when FEPIT exceeds about 40%. The

Table 1: Falstaff cases numbered by the solution and sphere numbers for the corresponding radius R_{sol}, steel vessel thickness d_{ss}, beryllium reflector thickness d_{Be}, and polyethylene thickness d_{Pe}, as applicable.

Case (No.)	Solution (No.)	Sphere (No.)	R_{sol} (cm)	d_{ss} (cm)	d_{Be} (cm)	d_{Pe} (cm)
1	4	1	7.8726	0.0483	9.1700	
2	4	2	8.5152	0.0483	6.5800	
3	4	3	9.0079	0.0483	5.2700	
4	4	3	9.0079	0.0483	1.1400	4.8800
5	4	4	9.6633	0.0483	3.8900	
6*	4	5	10.1625	0.0482	2.9000	
7	4	5	10.1625	0.0482	3.5700	
8*	4	6	10.7992	0.0483	1.9900	
9*	4	7	11.4152	0.0483	1.2400	
10	4	7	11.4152	0.0483	1.6800	
11	5	1	7.8726	0.0483	9.7300	
12	5	2	8.5152	0.0483	7.0900	
13	5	3	9.0079	0.0483	5.5900	
14	5	3	9.0079	0.0483	1.1400	6.2000
15	5	4	9.6633	0.0483	4.0900	
16	5	5	10.1625	0.0482	3.2000	
17	5	5	10.1625	0.0482	4.0400	
18*	5	6	10.7992	0.0483	2.0800	
19*	5	7	11.4152	0.0483	1.3700	
20	6	1	7.8726	0.0483	11.9100	
21	6	2	8.5152	0.0483	8.5300	
22	6	3	9.0079	0.0483	6.6800	
23	6	4	9.6633	0.0483	4.9000	
24	6	5	10.1625	0.0482	3.8200	
25	6	5	10.1625	0.0482	5.5100	
26	7	3	9.0079	0.0483	10.0800	
27	7	4	9.6633	0.0483	7.4900	
28	7	5	10.1625	0.0482	5.9200	
29	7	6	10.7992	0.0483	4.4200	
30	7	7	11.4152	0.0483	3.3000	
31	7	8	12.4564	0.0483	1.8400	

$*$ Large outliers in the benchmark calculations.

analysis indicates that the problem is very likely linked to the ^{233}U reaction cross sections. In Fig. 3 the results with the ENDF/B-VIII.0 ^{233}U evaluation (labeled **e80**) are compared to those using updated PFNS (labelled **e80u3a3**). The results indicate that the new PFNS causes a significant positive shift in reactivity, although the gradient as a function of FEPIT in these benchmarks with relatively hard neutron spectra remains practically the same.

3. Thermal Neutron Constants

The recommended Thermal Neutron Constants (TNC) [6] are shown in Table 2 compared to thermal values adopted in ENDF/B-VII.1 and ENDF/B-VIII.0 nuclear data libraries as well with the values adopted in the current evaluation. Note that the JEFF-3.3 library adopted the ENDF/B-VII.1 evaluation. The changes in capture cross section in ENDF/B-VIII.0 are greater than the reported uncertainty of the Standard TNC. The ^{233}U(n,f) cross section at thermal in the ENDF/B-VII.1 library is at the lower limit of the evaluated TNC which seems to be compensated by an overestimated total neutron multiplicity $\overline{\nu}_{tot}$. The thermal values adopted in the new evaluation are consistent with the new standards TNC evaluation well within the quoted uncertainties.

Table 2: The ^{233}U thermal neutron constants and their absolute uncertainties (in parentheses) are shown in the left column compared to the ENDF/B-VII.1 (center) and ENDF/B-VIII.0 (right column) adopted values. The thermal values of the current evaluation are reported in the last column.

Constant	Standard TNC	ENDF/B-VII.1	ENDF/B-VIII.0	Current
σ_{nf}(b)	533.0 (2.2)	531.3	534.1	532.2
$\sigma_{n\gamma}$(b)	44.9 (0.9)	45.3	42.3	44.6
σ_{nn}(b)	12.2 (0.7)	12.2	12.2	12.2
$\overline{\nu}_{tot}$	2.487 (.011)	2.497	2.485	2.487

4. Prompt Fission Neutron Spectrum

4.1. Thermal energy range

Simultaneous PFNS evaluations of thermal neutron–induced fission of ^{233}U, ^{235}U, and ^{239}Pu [12] were produced by using the least-squares GMA fitting

method [18, 19]. The measured data included in the fitting procedure were both absolute spectral data and data relative to the ^{252}Cf spontaneous fission reference spectrum, including the corresponding covariances evaluated by Mannhart [20, 21, 22]. The derived non-model evaluation (according to the classification discussed in Ref. [23]) was purely based on experimental data following the methodology developed in Ref. [24].

The resulting average energies of the PFNS evaluations for thermal neutron–induced fission were 2.000 ± 0.01 MeV for ^{235}U, 2.030 ± 0.013 MeV for ^{233}U, and 2.073 ± 0.01 MeV for ^{239}Pu thermal neutron–induced PFNS [12]. Those average energies were determined from about 25 keV up to 10 MeV of emitted fission neutrons, a range containing almost 99% of the spectra. Note that the derived PFNS average energies at the thermal point were about 30 keV lower than the energies used in previous ENDF/B libraries [3, 25] for these fissile targets.

Additional validation of the joint PFNS evaluation at the thermal point was provided by the excellent agreement with alternative evaluations of ^{235}U(n_{th},f) PFNS as discussed in Refs. [12, 26, 27]. The new ^{235}U(n_{th},f) PFNS was the one used in the CIELO project evaluation [28, 29, 30, 31, 32] that led to the new ^{235}U file adopted by the ENDF/B-VIII.0 library [4].

4.2. Fast energy range

The IAEA Coordinated Research Project on PFNS of major actinides [14] also included evaluations of the PFNS induced by fast neutrons in uranium and plutonium isotopes with up to 5 MeV of incident neutron energy, in particular in ^{233}U targets [13]. This evaluation was adopted for the current file for fast neutrons above the thermal point up to 5 MeV. Those evaluations were obtained using the Kalman filter [33], in conjunction with the Los Alamos model [34] predictions, as the prior information and experimental data sets used to update this information and thereby generate the posterior evaluated results. The only modification from the original Los Alamos model [34] was the introduction of non-isotropic emissions of the neutrons in the center-of-mass of the fission fragments. The resulting PFNS evaluations by Rising et al. [13] confirmed the

lower PFNS average energy derived independently by a non-model fit for all fissile isotopes [12].

5. *R*-matrix Analysis

5.1. Background

The resolved and unresolved resonance evaluations reported in the ENDF/B-VIII.0 library were performed in 2001 for the ENDF/B-VI.8 library and were successively adopted by the different releases of the ENDF library. With upper energy limits of 600 eV and 40 keV for the resolved and unresolved resonance ranges, RRR and URR, respectively, these evaluations followed the series of neutron transmission and fission measurements performed at ORELA. The accuracy of the resonance parameters and their averages resulted from the excellent experimental conditions of the newly measured ORNL neutron transmission and fission data. They were a large improvement compared with previous evaluations which, at that time, allowed accurate calculation of the cross sections over the energy range only up to 150 eV. In fact, to enable the *R*-matrix analysis over an extended energy range, the newly measured 80-meter-flight-path transmission data accounted for a highly enriched thick sample cooled to 11 K [10] and the fission measurements [9] for an experimental resolution better, by far, than any of the previous measurements [2]. However, after the ability of the evaluated cross sections to reproduce the effective multiplication factors k_{eff} for various thermal, intermediate and fast systems was tested, the average fission cross sections above 100 eV were based on the values of Weston's measured data [35, 36] to obtain better agreement with the intermediate energy systems. The discrepancy between ORELA average fission cross sections and the adopted measured data was not understood. Therefore, although the high-resolution data measured at

[2] The cooling of the sample was a technique used at the ORELA facility to reduce the resonance widths by decreasing the Doppler broadening by about a factor of 2 compared to measurements performed with a sample at room temperature. Due to the weak coupling of the atoms in the crystal assumed by the free gas model, an effective temperature (usually larger than the actual temperature) was used to numerically simulate the Doppler broadening of the measured resonances.

ORELA were essential to identify the systematics of the resonance parameters, the R-matrix analysis in the high-energy part of that work consisted of a shape-fitting analysis of the ORELA fission cross sections adjusted to other available measured data.

Almost a decade after the series of ORELA measurements and two releases of the ENDF library, a measurement of the ^{233}U fission cross sections [7] was independently performed at the neutron time-of-flight (n_TOF) facility at CERN. It showed agreement with previously measured ORELA fission data within 2% in the neutron energy range from 10 eV up to 100 keV. Moreover, benchmark calculations performed in view of the ENDF/B-VIII.0 release, and other independent criticality safety analyses, revealed a strong negative gradient of the effective multiplication factors k_{eff} for the thermal and intermediate energy configurations. In this regard, the adjustment of the ORELA fission cross section chosen in the previous evaluation seems to have been affected by a strong bias toward benchmarks sensitive to the intermediate energy region.

As a first step forward in resolving the poor systematics of the benchmark calculations, as predicted by the previous evaluation, the present work includes an updated R-matrix analysis consistent with the newly evaluated constant values in the thermal neutron region and the ORELA fission cross sections in the neutron energy region above 100 eV. Moreover, both the definition of the R-matrix external function with related covariance quantification and the analyses of both ORELA transmission and fission data sets in the neutron energy region above 600 eV, in relation to their specific experimental conditions, are discussed as a fundamental step for further extension of the resolved resonance range.

5.2. External R-matrix function

The definition of the energy levels and corresponding reaction resonance widths in the energy region below and above the limits of any multi-channel R-matrix analysis is of fundamental importance. The negative levels are usually referred to "bound levels," and the related resonance parameters are highly sensitive to the reaction cross sections in the thermal energy range and below.

In the particular case of fissile actinides with small average level spacing typical of odd-A nuclei such as ^{233}U and ^{235}U, the analysis of the negative levels requires particular attention. The reason is that the resonance parameters for negative levels close to zero are crucial to fitting both the measured energy (positive) levels close to zero—i.e., below 0.5 eV—and the fission and capture reaction channels that, in the thermal energy region, define almost entirely the magnitude of the total cross section. In this regard and within the limits of this subsection, the definition of the external R-matrix function and correlations among the reaction cross sections are analyzed.

Among the several methodologies used for defining the energy-dependent contribution of the external levels, the definition of fictitious external resonances based on the systematics of the fitted resonance parameters is a convenient method often used in nuclear data evaluations. Similarly, the external R-matrix function originated from the statistical properties of the resonance parameters; but it was defined by the average reaction cross sections reconstructed from sets of resonance parameters and energy and reaction (neutron and fission) widths, randomly sampled from the Wigner and Porter-Thomas distributions, respectively. The random sampling of the resonance parameters and the related average of the reaction cross section are thought to account for the large variations of the external R-matrix function due to the closeness of negative levels to the zero energy.

In Fig. 4, the n+^{233}U average reaction cross sections reconstructed from 100 sets of resonance parameters randomly sampled and defined over the energy regions between -600–0 eV and 600–2500 eV are shown as solid lines for each reaction channel and compared with the external R-matrix function reported in the ENDF/B-VIII.0 evaluation plotted as dashed lines. According to the Wigner distribution for the two s-wave J-spin populations used for sampling the energy levels,the level spacings are $D_{0,2^+} = 1.95$ eV and $D_{0,3^+} = 1.40$ eV. In the R-matrix framework of the Reich-Moore approximation, the capture width was kept constant at $\Gamma^\gamma = 39$ meV. Within the Porter-Thomas distribution with degree of freedom $\nu = 1$, the adopted neutron widths for the sampling were

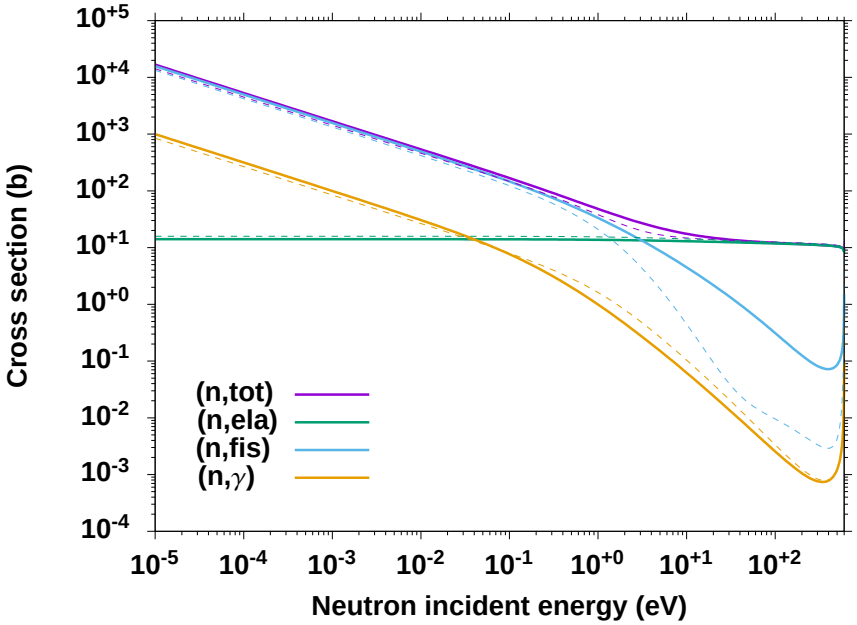

Figure 4: The n+^{233}U average reaction cross sections reconstructed by sampling 100 sets of resonance parameters are shown as solid lines. The reconstructed cross sections taken from the ENDF evaluation are plotted as dashed lines.

$\Gamma^{n}_{0,2^+} = 0.21$ meV and $\Gamma^{n}_{0,3^+} = 0.14$ meV. With the same degree of freedom, the values of the fission widths were assumed to be the same for both channels and were $\Gamma^{f_{1,2}}_{0,2^+} = 1300$ meV and $\Gamma^{f_{1,2}}_{0,3^+} = 880$ meV. As expected, the elastic cross section for both cases was constant over almost the entire energy range. Reflected in an increased total cross section with respect to ENDF/B-VIII.0, the largest deviations were visible for the capture cross sections below 1 eV and the fission reaction channel above 0.1 eV. With the generated R-matrix external function, the fraction of the thermal constant values to the total value for each reaction channel can be estimated. These were about 57% and 42% for the fission and capture channels, respectively. Above 300 eV, the anti-correlation between the elastic and reaction (fission and capture) channels was also evident and was confirmed by the cross-reaction correlation matrices shown in Fig. 5. The reaction-reaction matrix of all channels shows strong, positive, long-range correlations up to 300 eV. Above that, the correlations are still large but are

uncorrelated or slightly anti-correlated with the region below. The covariance analysis shows extremely large uncertainty (above 100%) associated with the calculated average cross sections in the low-energy range up to a few eV. This is explained by the large sensitivity of the different randomly sampled sets of resonance parameters affecting the low-energy tail of the fission and capture cross sections.

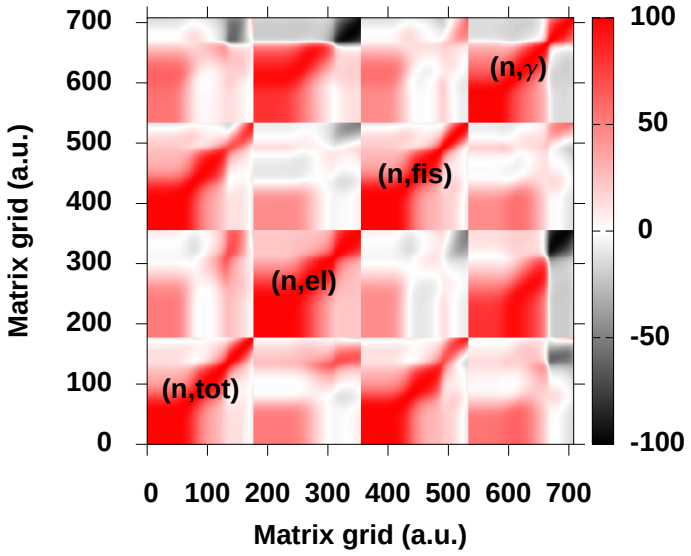

Figure 5: Correlation matrices of n+^{233}U average reaction cross sections reconstructed by sampling 100 sets of resonance parameters are shown in palette colors from fully negative correlation (in black) gradually to fully positive correlation (in red).

The reported covariance analysis of the R-matrix external function depends greatly on the choice of statistical properties of the resonance parameters, i.e., level spacing and average reaction widths. However, the large cross section correlations defined by the resonance parameters of this function, coupled to the extremely large sensitivity of the resonance parameters related to the level spacing, are a common feature in the R-matrix theoretical framework. As a relevant step in the evaluation procedure, this is particularly important for the uncertainty quantification of the resonance parameters defined for negative energies

in relation to the optimization techniques used to fit the available measured data sets, including thermal constant values.

5.3. Current updates up to 600 eV

A preliminary set of resonance parameters for more than 700 levels was obtained in the neutron energy range between thermal and 600 eV by the fit of selected transmission, fission, and capture measured data. Starting from the values of the resonance parameters reported in the ENDF/B-VIII.0 library, the first step of the evaluation process was to recalibrate the fission cross sections in the energy region above 50 eV to the average values reported in the ORELA and nTOF fission data measured by Guber and Calviani, respectively, as shown in Fig. 6. In contrast with the Weston simultaneous fission and capture measurements were limited to 2 keV, the ORELA and nTOF fission data were measured over an extensive energy range. Accordingly, these two data sets become very important to guarantee compatibility between RRR and URR, although the lack of a simultaneous measurement related to the capture reaction channels as performed by Weston would have been ideal for the current analysis. Although a direct comparison with the measured data was not possible owing to the different experimental conditions, a systematic increase in the average fission cross sections was reported by both measurements. This increase was reproduced relatively well by the calculated average cross sections reconstructed from the newly updated set of resonance parameters. To perform a meaningful comparison with the measured data as shown in Fig. 7, the calculations were obtained by the convolution of the theoretical cross sections calculated from the selected resonance parameters and the experimental conditions such as Doppler and resolution broadening, as well as the corresponding experimental energy binning.

The second step of the evaluation process was to incorporate the thermal constant values newly evaluated by the IAEA project in standards cross sections for the elastic, fission, and capture reaction channels. As shown in Fig. 6, several measured data sets—such as Moore [37] and Pattendend [38] for the

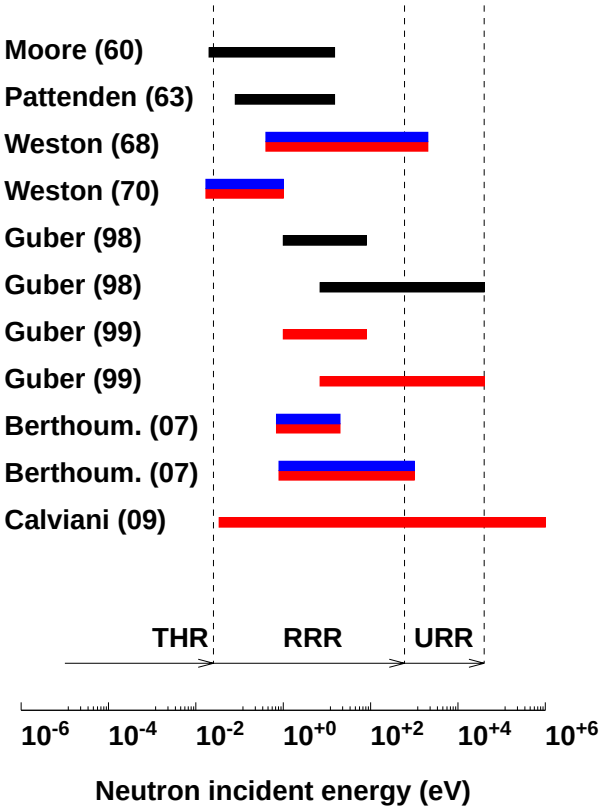

Figure 6: Experimental database for selected measured data with corresponding energy range. The total/transmission data sets are shown in black and the fission and capture data in red and blue, respectively. Experimental data featuring the simultaneous measurement of fission and capture reaction channels are shown with joint colored bands.

total cross sections and Weston [35, 36] for both fission and capture extended over the thermal and low-energy region— were scaled according to their isotopic enrichment to the newly evaluated standards thermal values for consistency. The preliminary sequential fit of the selected measured data, including thermal constant values from the standards, yielded thermal constant values (calculated at T=0 K) +0.6% and +3% for the elastic and capture channels higher than the ENDF/B-VIII.0 evaluation, and -0.2% lower for the fission reaction channel.

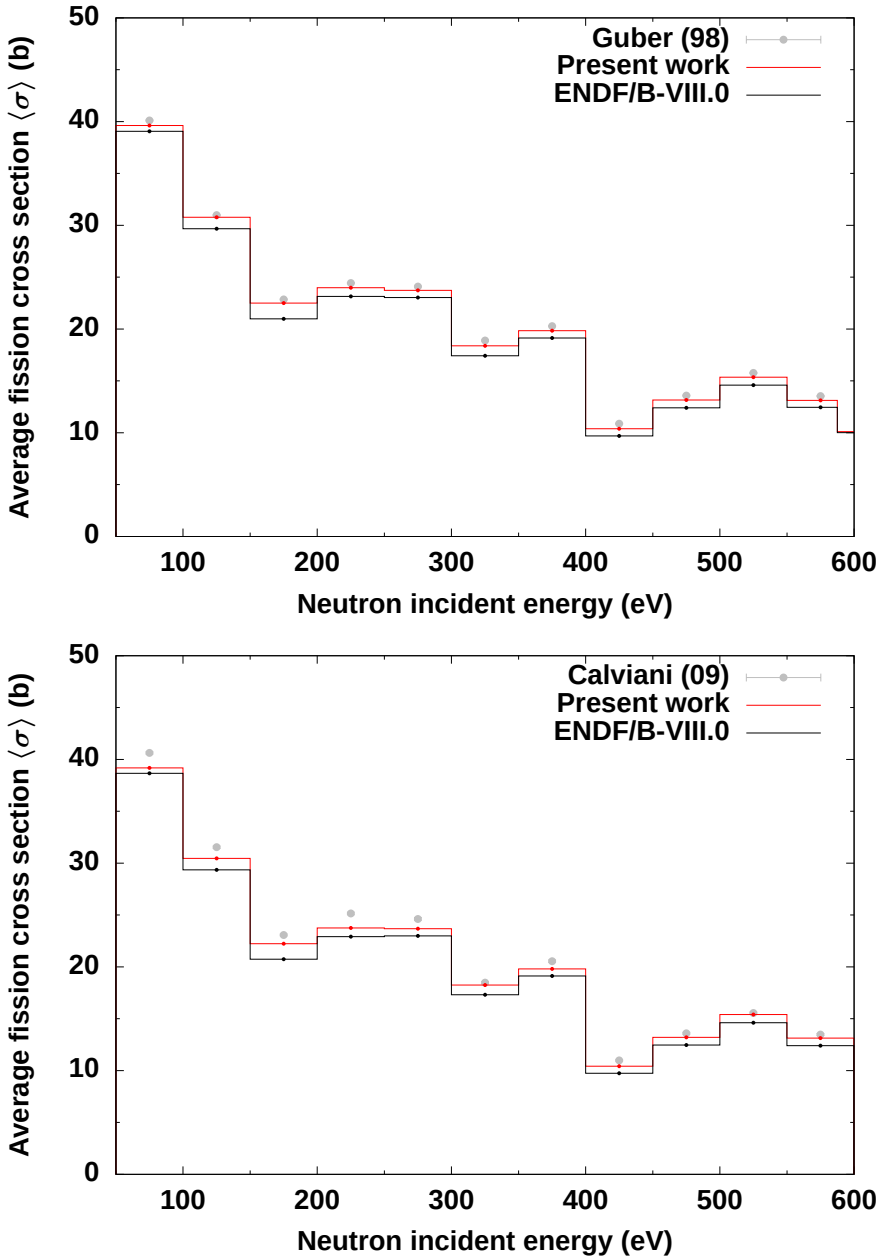

Figure 7: Average measured fission cross sections compared with the values calculated from the ENDF/B-VIII.0 resonance parameter and present work. The calculated values include experimental corrections such as Doppler and resolution broadening, as well as the corresponding experimental energy binning.

These changes left the total cross section almost unchanged. The result of the preliminary sequential fit with available measured data for the total, fission, and capture reaction channels is shown in Fig. 8.

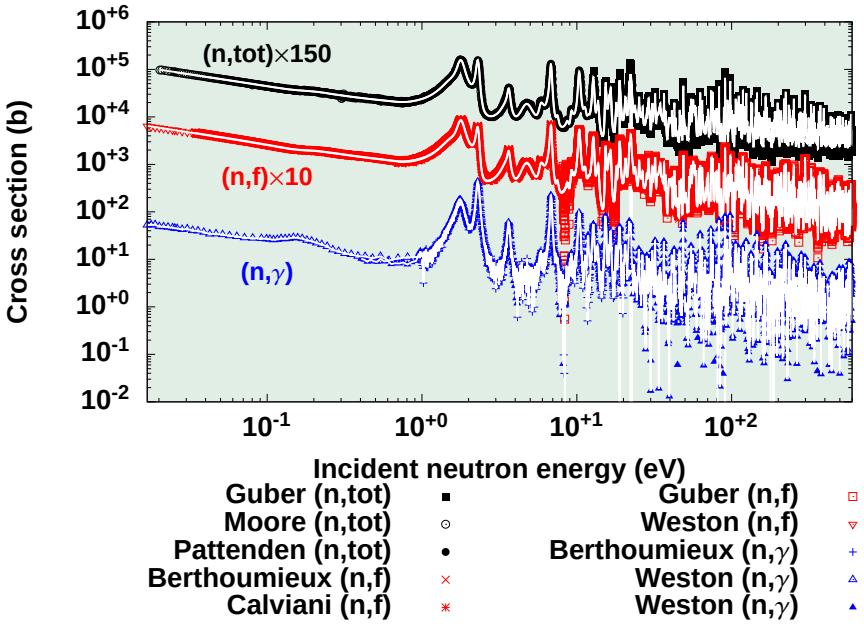

Figure 8: Comparison between measured and calculated cross sections for total, fission, and capture cross sections in the energy range between 0 and 600 eV. The plotted data sets are scaled for visibility purposes.

For the ^{233}U evaluation, the fit-shape analysis of the fission and capture cross sections below 0.2 eV required particular attention because of the low-lying level at about 0.17 eV and the high sensitivity related to the criticality benchmarks. Well defined in the experimental capture cross sections, this level is seen as a small interference deformation in other measured data, such as the total and fission reaction channel. Although further analysis is needed, this work adopted the resonance parameter configuration of the ENDF/B-VIII.0 evaluation, consisting of a description of the resonance capture near 0.2 eV as a doublet slightly below and above that energy region. Some of the difficulties in describing the low-energy range relate to the very small capture width and the correlation between the fission and capture channels. In this regard, the uncertainty as-

sociated with the capture and fission measured data considerably affected the results of the optimization procedure. In fact, although the reasonable fit obtained in the sequential optimization procedure of the measured data as shown in Fig. 9, the current fit is still unable to accurately describe the low-lying resonance for the fission channel by using the cross section uncertainty provided by the measured data.

5.4. Future updates above 600 eV

In addition to our results for the observed neutron resonance energies up to 600 eV, the availability of total and fission measured data up to the first inelastic state at 40.35 keV is very valuable information; it could be used for further extension of the evaluation in the RRR as well as the quantification of the average reaction cross sections in the URR. In this regard, Guber's measurements performed at ORELA in the late 1990s represent the most suitable experimental database for this analysis because of their extremely high resolution for the total and fission reaction channel that, in magnitude, is the dominant reaction process.

The R-matrix analysis to extend the RRR evaluation up to 2.5 keV was initiated, with the fit of the Guber transmission data and fission cross sections following the generation of populations of energy levels and resonance parameters sampled from the Wigner and Porter-Thomas distributions, respectively, for the two compound-nuclear states of positive parity, $J = 2^+$ and $J = 3^+$. The results of the fit up to 2.5 keV are shown in Fig. 10, for which the capture reaction channel is described by the Weston data [35] with an average capture width of 39 meV, according to the Reich-Moore approximation. The systematics of the resonance levels obtained after the fit of the measured data up to 2.5 keV are shown in Figs. 11–12.

Figure 11 shows the cumulative number of observed and predicted resonance levels $N \gtrsim 3000$ versus the incident neutron energy E for ^{233}U. The figure shows a nearly linear slope that extends to about 2.5 keV. It indicates that in the vast majority of our reported levels, both strong and narrow weak s-levels were

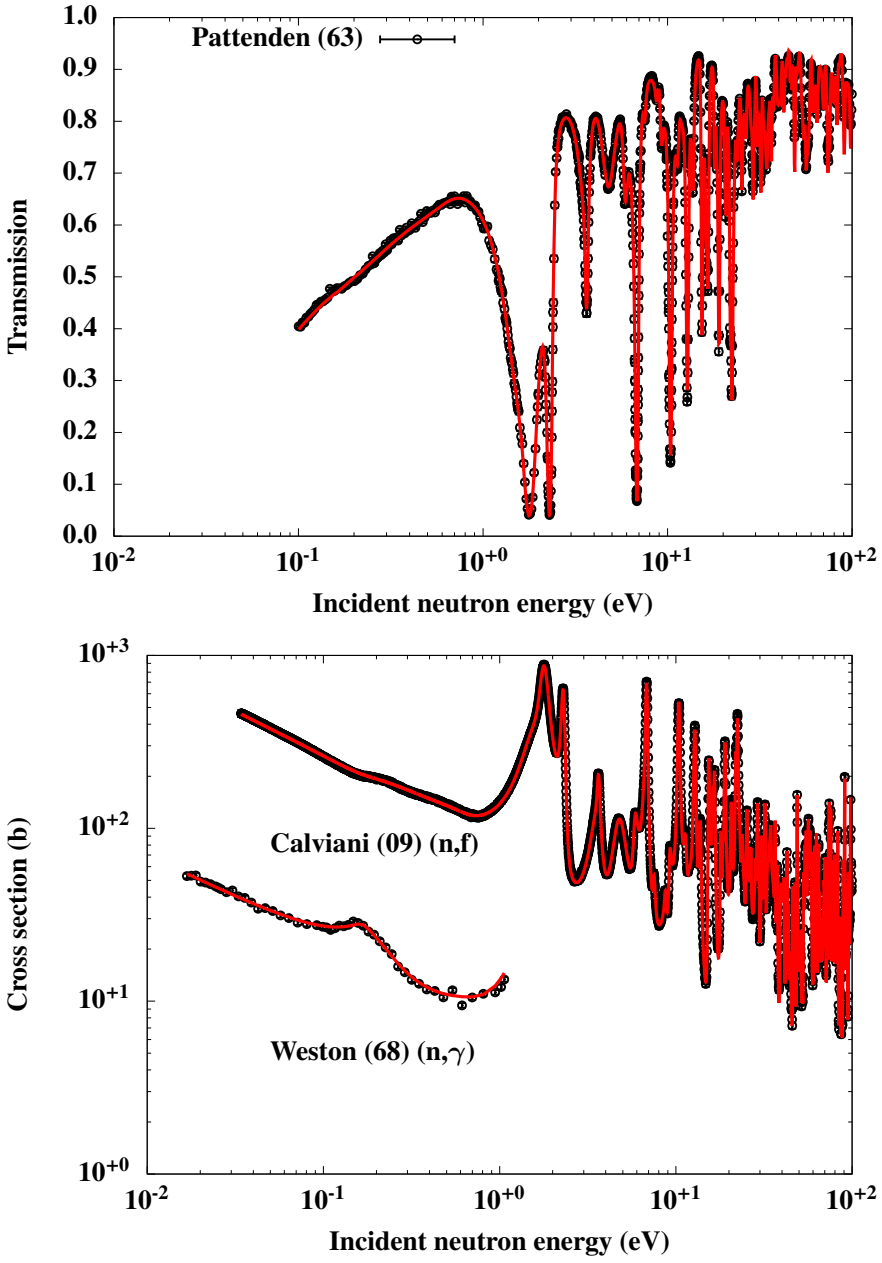

Figure 9: Comparison between measured and calculated cross sections for total (Pattenden), fission (Calviani), and capture (Weston) cross sections in the energy range between 0 and 100 eV.

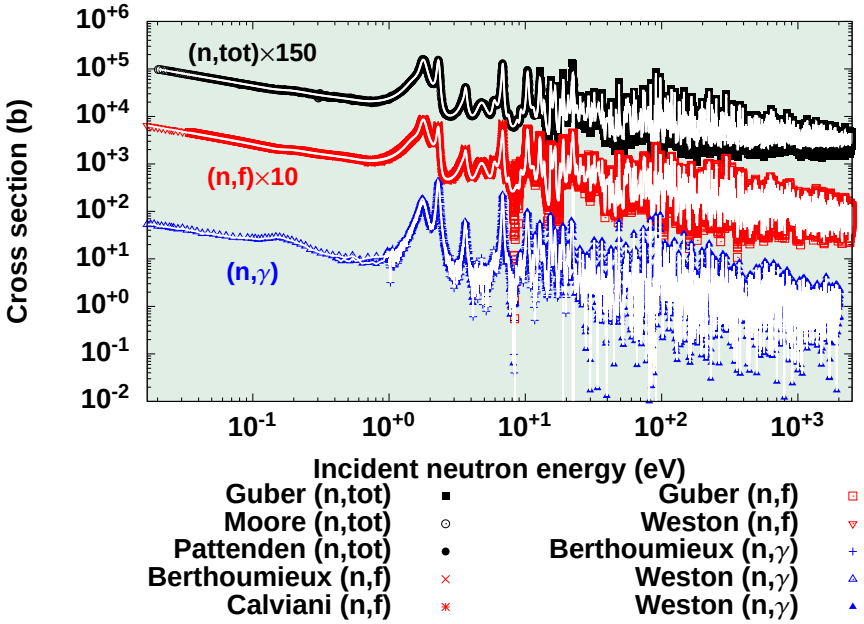

Figure 10: Comparison between measured and calculated cross section for total, fission, and capture cross sections in the energy range between 0 and 2.5 keV. The plotted data sets are scaled for visibility purposes.

included in the set of initial resonance parameters. The figure includes various fitted straight lines, which imply mean s-level spacings $\langle D_{l,J}\rangle$ for partial (green and purple dots) and mixed populations (blue dots). As expected, the $\langle D_l\rangle$ of ^{233}U tends to be much smaller than that of even-A isotopes, since ^{233}U has two randomly mixed independent populations.

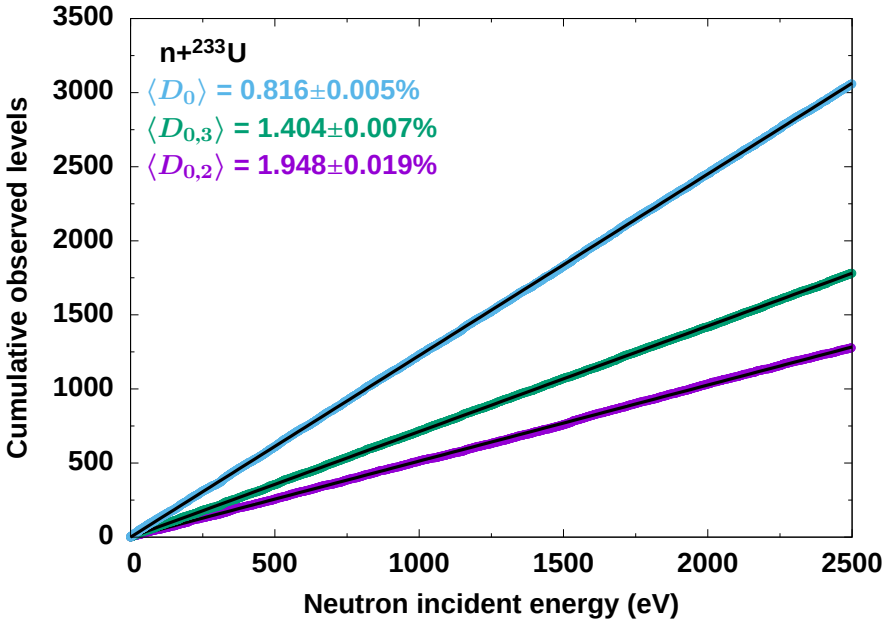

Figure 11: Plot of the cumulative number of observed s-levels (blue dots) vs energy for n+^{233}U. The values of average s-level spacings for two J-spin populations, $\langle D_l\rangle$, and the mixed population, $\langle D_{l,J}\rangle$, shown in the plot represent the inverse of the slope of a straight line (in black) fitted to the data (green and purple dots).

Figure 12 graphs the cumulative reduced neutron widths $\Gamma^{0\ell}_{n,\lambda}$ related to the neutron width by $\Gamma^{0\ell}_{n,\lambda} = \Gamma^{\ell}_{n,\lambda}\sqrt{1\text{ eV}/E_\lambda}$, where $v_\ell(E_\lambda) = P_\ell(E_\lambda)/P_0(E_\lambda)$ is the normalized centrifugal-barrier penetration factor (unitary for s-wave). The slope of the plot obtained by the best fit of the reduced neutron widths (colored dots) corresponds to the $S_{\ell,J}$ neutron strength function for each population and mixed populations. From the fitted values of the neutron strength functions for each population, there is a weak J-dependence.

The analysis of the statistical properties of the resonance parameters (en-

ergy levels and reaction widths) is useful as a test of the nuclear reaction theory in particular. Therefore, a comprehensive analysis of the systematics of observed s-wave resonances should also include comparisons with known Gaussian Orthogonal Ensemble (GOE) distributions, e.g., comparisons of the calculated reduced (neutron and fission) widths within the Porter-Thomas distribution and the energy levels within the Wigner distribution as shown in Figs. 13–15.

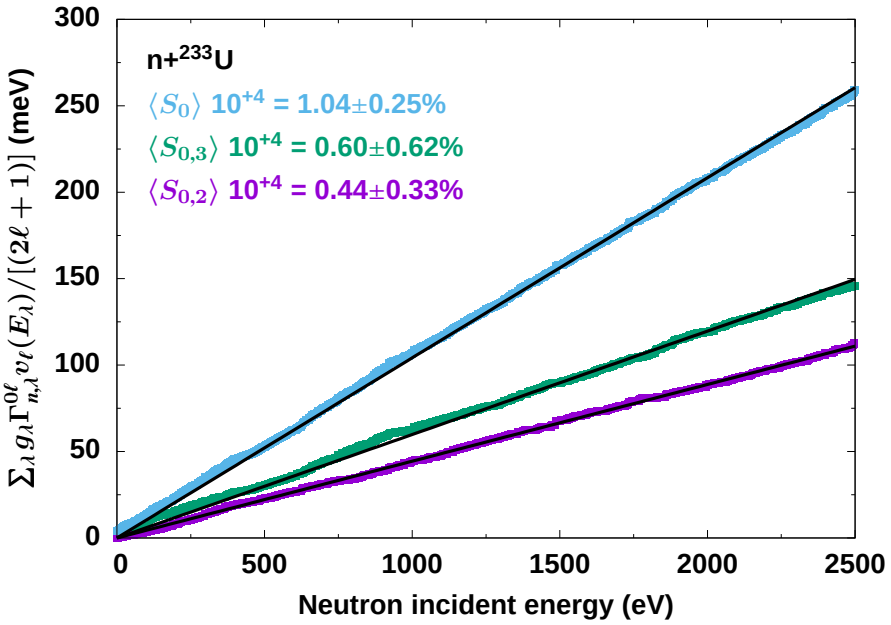

Figure 12: Plot of the cumulative reduced neutron-widths of observed s-levels (blue dots) vs. energy for n+^{233}U. The slopes of the straight lines give the strength function $S_{0,J}$ (in 10^{+4} unit).

In the figures, a slight deviation from the theoretical distributions is noticed that is prominent mainly for the values of the distributions near zero. This might indicate an overestimation of the very narrow levels with very small widths for both neutron and fission channels, and it might be understood by the tendency of the fitting procedure to fit clusters of resonances instead of resonance levels with well-resolved neutron and fission widths. Additional work is in progress to verify this hypothesis and improve the agreement with the theoretical distributions as an important constraint in the extension of any R-matrix analysis.

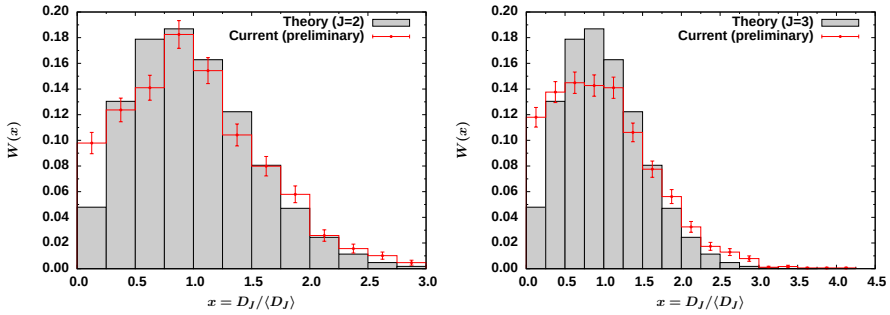

Figure 13: The results of the nearest-neighbor-spacing distribution (in red) are compared with the Wigner distribution (in black and gray histograms) normalized to unity for ℓ=0 and J-spin populations $J = 2^+, 3^+$. The dimensionless variable x is defined by the ratio of the nearest-neighbor and average ℓ-wave level spacing, respectively

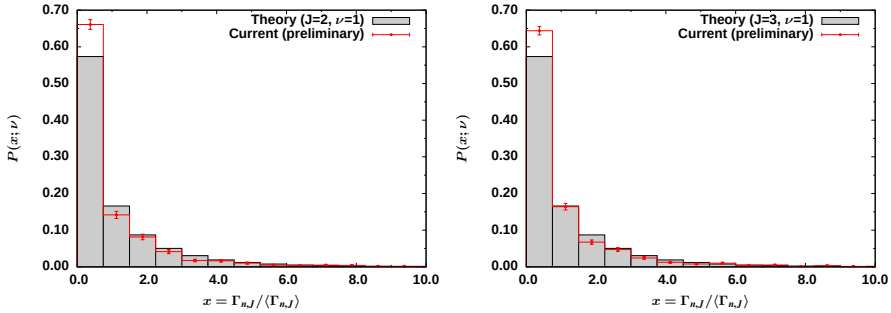

Figure 14: The results of the Porter-Thomas distribution (in red) are compared with the theoretical distribution (in black and gray histograms) normalized to unity for ℓ=0 and J-spin populations $J = 2^+, 3^+$. The dimensionless variable x is defined by the ratio of the ℓ-wave neutron width and its average, respectively

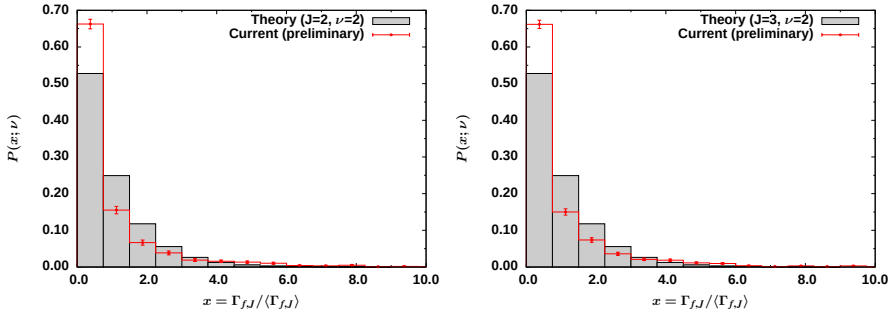

Figure 15: The results of the Porter-Thomas distribution (in red) are compared with the theoretical distribution (in black and gray histograms) normalized to unity for ℓ=0 and J-spin populations $J = 2^+, 3^+$. The dimensionless variable x is defined by the ratio of the ℓ-wave fission width and its average, respectively

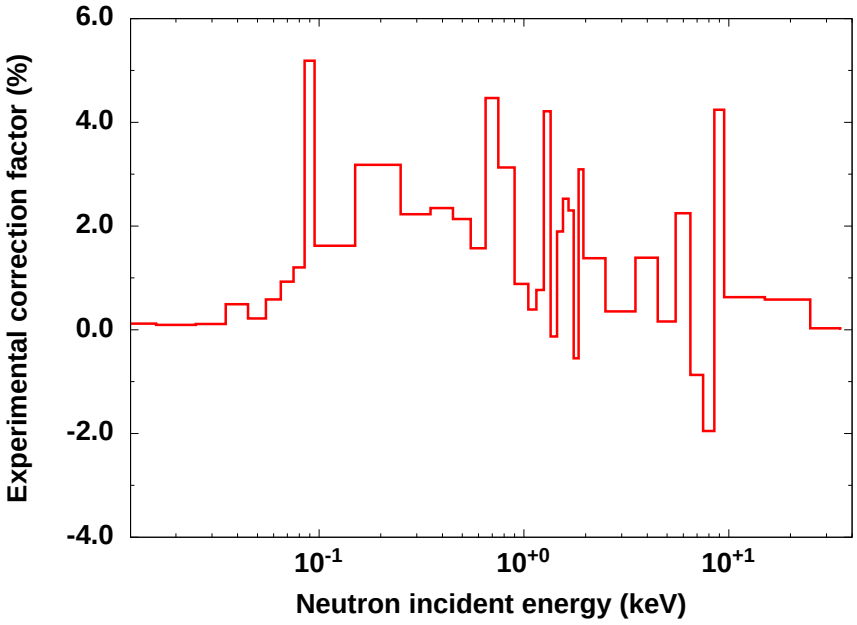

Figure 16: Average and energy-dependent experimental corrections factor related to Guber's transmission measured data in the neutron energy range up to 40 keV.

As an additional and important step in the procedure to extend and evaluate the reaction cross sections in the URR, quantification of the experimental corrections, such as Doppler and resolution broadening, is needed. In the specific case of the total and fission cross sections, Guber's transmission and fission data measured at ORELA are suitable for this task because both data sets extend up to 40 keV. An example of the average and energy-dependent experimental correction factors for the total reaction channel is shown in Fig. 16, where the correction factor is estimated at between 2 and 5%. It was calculated by comparing the theoretical cross sections and their convolution with the calculable experimental corrections. The calculation of the cross sections over such a large energy range above 2.5 keV was possible by generating randomly sampled populations of resonance parameters between 2.5 and 40 keV according to the usual distributions. This approach represents an important step toward including the most updated and comprehensive experimental information in future releases of

the ENDF/B library.

6. Benchmark Analysis of the Updated Evaluation

The new resonance file extending up to 600 eV was integrated into the updated ^{233}U evaluation (**e80u3a3**) to become the new ^{233}U evaluated file discussed in this work (**e80u3a506c**), and selected solution benchmarks were executed to check the impact. The following benchmarks from the ICSBEP Handbook were considered to evaluate the performance of changes in the thermal and epithermal region:

- U233-SOL-THERM-[001, -008, -009] unreflected nitrate solutions
- U233-SOL-THERM-005 water-reflected nitrate solutions
- U233-SOL-THERM-015 uranyl-fluoride solutions with different reflectors

We excluded the U233-SOL-THERM-012 water-reflected and U233-SOL-THERM-013 unreflected cases from Oak Ridge because we could not explain the high reactivity prediction, which is contradictory to other benchmarks. All other ^{233}U benchmarks in the ICSBEP Handbook include other reflector materials or ^{233}U solution vessels immersed in water, which would require extensive sensitivity studies to determine the possible impact of additional materials and additional geometrical complexity. In Fig. 17 we check the impact of the following changes to the original ENDF/B-VIII.0 evaluation (labeled "e80"):

- The PFNS from the evaluation with Standards-2017 for incident thermal neutrons and the PFNS by Rising [13] from the IAEA CRP [14] (label "**e80u3a3**")
- Changes in the previous item plus new resonance parameters from ORNL (labeled "**e80u3a506c**")

Figure 17 shows that the strong negative gradient observed with ENDF/B-VIII.0 evaluation is greatly reduced by the softer PFNS spectrum. The new ORNL resonance parameters further reduce the gradient, although some underestimation

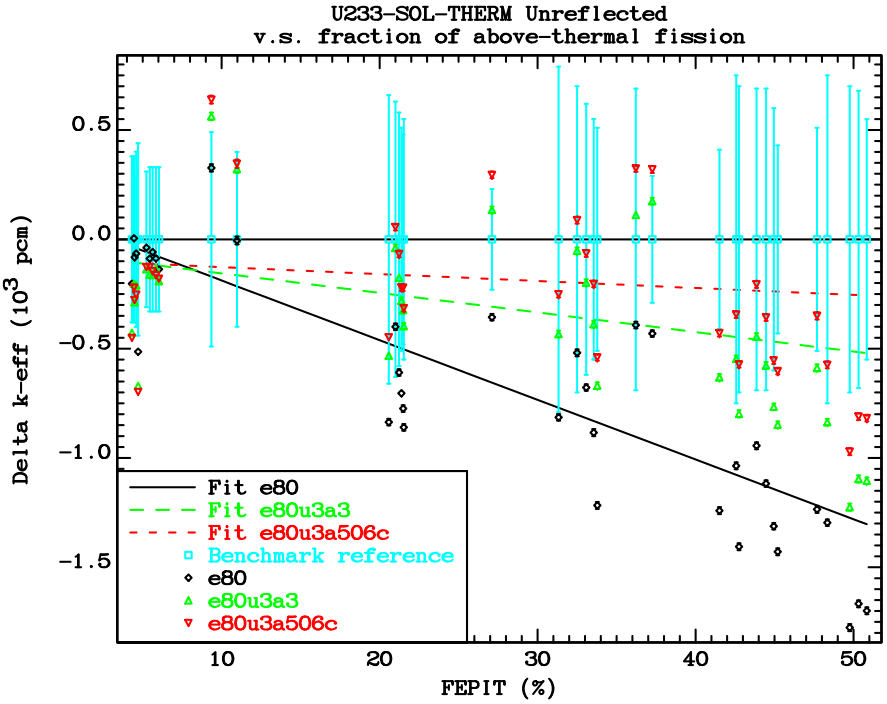

Figure 17: Selected ^{233}U solution-benchmark results with updated PFNS (**e80u3a3**) and updated PFNS and resonance data (**e80u3a506c**) compared with ENDF/B-VIII.0 (e80) results.

of reactivity begins to appear at FEPIT values greater than 40 %. The overall situation of the benchmark results is shown in Fig. 18. The comparison includes the ENDF/B-VII.1 library (label "e71"); the ENDF/B-VIII.0 library (labeled "e80"); the ^{233}U evaluation from this work (labeled "**e80u3a506c**"); and the full suite of INDEN evaluations, which include improvements to chromium (new evaluation), iron (corrections to ^{56}Fe from ENDF/B-VIII.0), oxygen (including correction to JENDL-4/HE), fluorine (adopted from JENDL-4/HE), and the ^{233}U evaluation from this work (labeled "**e80Fe_X29r39ojCrKUW**"). Figure 18 shows that the trend observed in ENDF/B-VIII.0 is similar to that seen in ENDF/B-VII.1, except for some additional negative shift in reactivity. The impact of the other INDEN evaluations is a positive shift in reactivity (comparing **e80Fe_X29r39ojCrKUW** with **e80u3a506c**), which happens to match the benchmark values almost perfectly. The largest impact of the new INDEN

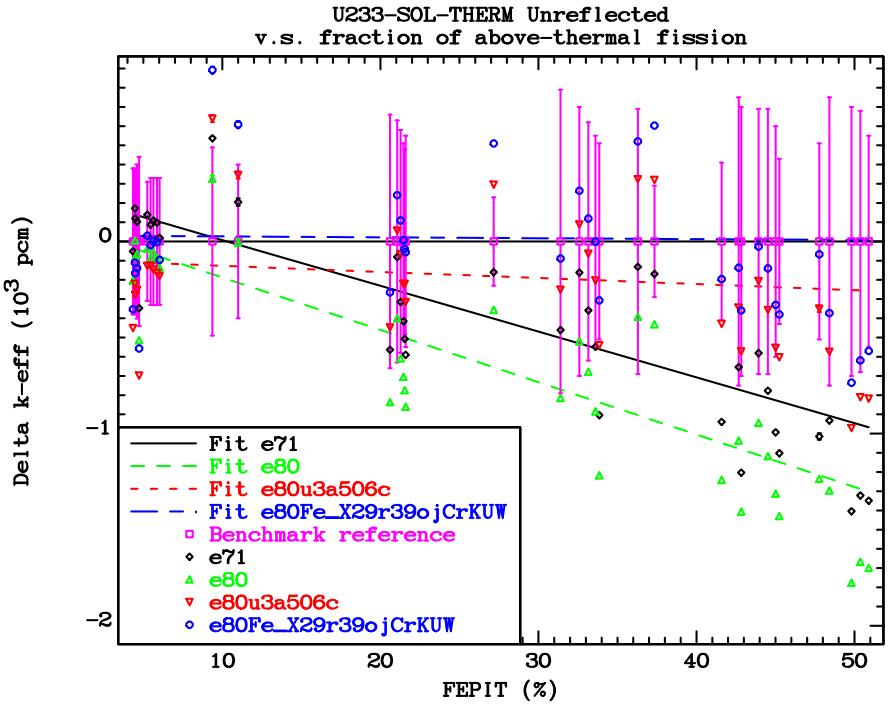

Figure 18: Selected ^{233}U solution-benchmark results with improved evaluations (**e80u3a506c** and full INDEN **e80Fe_X29r39ojCrKUW**) compared with previous ENDF/B-VII.1 (e71) and ENDF/B-VIII.0 (e80) results.

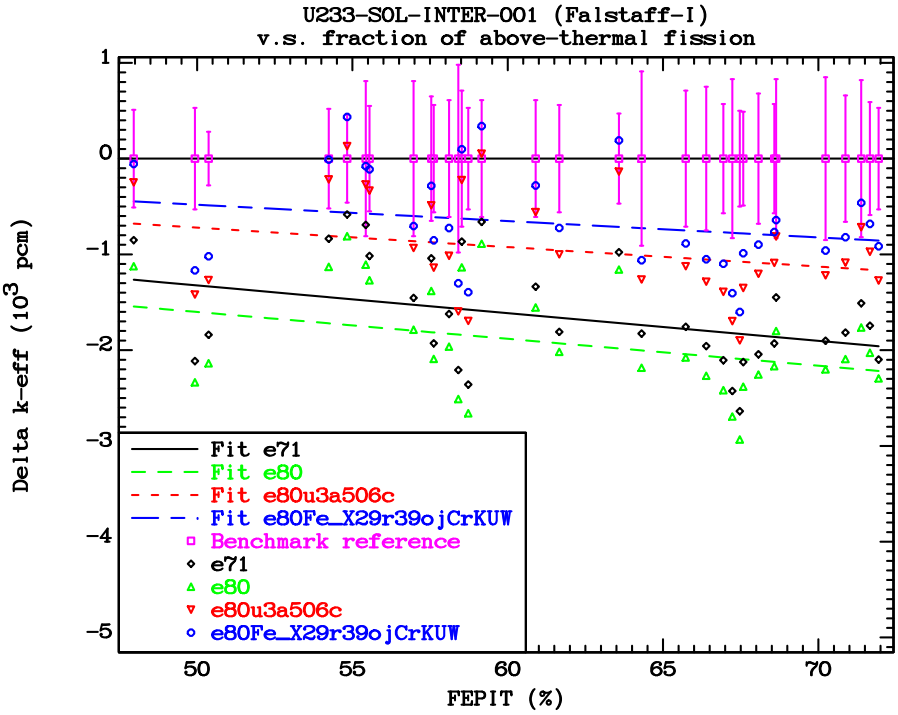

Figure 19: ^{233}U benchmark results with improved evaluations (**e80u3a506c** and full INDEN **e80Fe_X29r39ojCrKUW**) compared with previous ENDF/B-VII.1 (e71) and ENDF/B-VIII.0 (e80) results for the U233-SOL-INTER-001 benchmark (many cases).

evaluations on this group of ^{233}U solution benchmarks is due to the reduced absorption in the adopted JENDL-4/HE evaluation of ^{16}O.

To gain more insight into the performance of the ^{233}U evaluation in intermediate neutron spectra, the U233-SOL-INTER-001 group of benchmarks from the Falstaff program at Lawrence Livermore National Laboratory was analyzed. Unfortunately, there are no similar highly enriched uranium benchmarks for an intermediate neutron spectrum. The U233-SOL-INTER-001 group of benchmarks is complementary to the U233-SOL-THERM-015 group of benchmarks from the same laboratory undertaken in the same installation. The results are shown in Fig. 19. From the figure it is seen that the covered FEPIT range extends from 50 % to 75 %. The reactivity trends are consistent with the U233-SOL-THERM-015 in the sense that the reactivity trends are just extrapolations to higher FEPIT values with approximately the same gradient. Some small

negative bias is observed, but there are large fluctuations among benchmark cases with different FEPIT values.

In spite of the excellent benchmark results shown in this section, it should be mentioned that at least two groups of benchmarks (U233-SOL-THERM-012 and U233-SOL-THERM-013) show significantly higher reactivity. There are also benchmarks involving other materials, which have not been analyzed in detail. Finally, there are always possibilities of systematic errors in individual groups of benchmarks.

7. Summary and Conclusions

Following poor benchmark performance for thermal solutions of the ^{233}U evaluation observed in both ENDF/B-VII.1 and ENDF/B-VIII.0 releases of the US nuclear data library [3, 4], this paper first reported an analysis of the systematics of the calculated and measured k_{eff} for ^{233}U solutions. Large outliers in the benchmark calculations were identified as related to spherical thermal solution benchmarks with beryllium reflectors thinner than 3 cm.

However, once those outliers were removed, the problem of underestimated reactivity was still most likely to be linked to deficiencies in the evaluated cross sections and fission neutron spectra.

Following the updates in ^{233}U evaluations using differential data for both thermal cross sections and multiplicities as well as PFNS, a new evaluation of resonance parameters using all existing experimental data normalized to the IAEA 2017 TNC was undertaken.

Available PFNS evaluations produced within the IAEA CRP [14, 12] were used to replace existing PFNS evaluation in the ENDF/B-VIII.0 library up to 5 MeV. A lower average energy of the PFNS evaluation at the thermal point induced a shift in reactivity of about +500 pcm, which improved benchmark performance but did not eliminate fully the observed trend vs. the epithermal fraction (FEPIT).

In the evaluation of resonance parameters within the *R*-matrix Reich-Moore approximation for *s*-wave–induced neutron energies in the ^{233}U nucleus—within

the energy range from thermal up to different energy ranges obtained from the SAMMY analysis of a selected experimental database—the first step of the analysis was devoted to recalibration of the fission cross sections to ORELA and nTOF measured data, as well as incorporation of the newly evaluated thermal constant values [6]. Since several data sets extended from the thermal region, these were renormalized consistently to the new thermal values. As shown in Fig. 6, the experimental database is comprehensive in all reaction channels up to 2 keV.

Based on the statistical properties of the resonance parameters, this work reports the quantification of the external R-matrix function and the correlations among the available reaction channels. As defined in this paper, the external function is highly correlated, as well as highly uncertain, for very small neutron energies. This analysis attempted to establish a consistent procedure for defining the external levels and related covariances. A preliminary evaluation e80u3a506c was released up to 600 eV. Additional work for a possible extension of the RRR evaluation to 2.5 keV, which is also related to the evaluation of the URR up to 40 keV, was discussed, together with the experimental corrections factor needed for the evaluation procedure. Moreover, future updates to the R-matrix evaluation should include, when available, newly measured α-ratio data [15]. As previous measurements performed by Weston [35], simultaneous measurements on ^{233}U nucleus are characterized by the challenge to accurately distinguish between capture and fission γ-rays when the capture events are considerably smaller than the fission events. Consistency between neutron multiplicity and R-matrix evaluation should be also achieved as a step forward.

A newly assembled evaluated ^{233}U file was made available through the INDEN collaboration[3]. The unreflected solution benchmark performance of this file shows a significant improvement over previous ENDF/B evaluations, and the new file combined with other updated INDEN evaluations shows practically no trend as a function of FEPIT for the selected set of ^{233}U solution bench-

[3]Available at the INDEN webpage https://www-nds.iaea.org/INDEN/, May 15,2020

marks. A critical review of additionally available ^{233}U solution benchmarks is desirable. Further evaluation work addressing both the resonance and the fast neutron regions is warranted.

Acknowledgments

This work was supported by the Nuclear Criticality Safety Program, funded and managed by the National Nuclear Security Administration for the Department of Energy.

The authors would like to acknowledge very useful discussions on ^{233}U benchmarks held with A.C. (Skip) Kahler.

To Max Salvatores,

MP had the pleasure to meet first Max in 2007 while working on the generation of an extensive set of covariances for future releases of the US ENDF library. This was the beginning of a very fruitful collaboration with Max within projects focusing on data adjustment—such as the Global Nuclear Energy Partnership and programs such as the Nuclear Criticality Safety Program that, at that time, addressed the scarcity of neutron covariance data with the joint efforts of four major US national laboratories (Brookhaven National Laboratory, ORNL, Los Alamos National Laboratory, and Argonne National Laboratory). The collaboration with Max peaked in the use of covariance matrices in a consistent multiscale data assimilation, a project based on Max's idea to use basic nuclear model parameters and related covariance information to improve the agreement with integral data experiments: from meters to femtometers.

Particularly important in the early stage of a career in the nuclear data field, Max clearly taught MP the equal importance of the physics that intrinsically supports the applied world, as well as the pragmatism necessary to move forward and make the applied world more and more reliable.

[1] R. Capote, L. Leal, Liu P., Liu T., P. Schillebeeckx, M. Sin, I. Sirakov, and A. Trkov. Evaluated Nuclear Data For Nuclides Within The Thorium-Uranium Fuel Cycle. Technical Report STI/PUB/1435, International Atomic Energy Agency, 2010. URL http://www-nds.iaea.org/reports-new/tecdocs/sti-pub-1435.pdf.

[2] R. Capote Noy. Summary Report of IAEA Consultants Meeting on Review Benchmarking of Nuclear Data for the Th/U Fuel Cycle. Technical Report INDC(NDS)-0586, International Atomic Energy Agency, 2011.

[3] M. B. Chadwick, M. Herman, P. Obložinský, M. E. Dunn, Y. Danon, A. C. Kahler, D. L. Smith, B. Pritychenko, G. Arbanas, R. Arcilla, R. Brewer, D. A. Brown, R. Capote, A. D. Carlson, Y. S. Cho, H. Derrien, K. Guber, G. M. Hale, S. Hoblit, S. Holloway, T. D. Johnson, T. Kawano, B. C. Kiedrowski, H. Kim, S. Kunieda, N. M. Larson, L. Leal, J. P. Lestone, R. C. Little, E. A. McCutchan, R. E. MacFarlane, M. MacInnes, C. M. Mattoon, R. D. McKnight, S. F. Mughabghab, G. P. A. Nobre, G. Palmiotti, A. Palumbo, M. T. Pigni, V. G. Pronyaev, R. O. Sayer, A. A. Sonzogni, N. C. Summers, P. Talou, I. J. Thompson, A. Trkov, R. L. Vogt, S. C. van der Marck, A. Wallner, M. C. White, D. Wiarda, and P. G. Young. ENDF/B-VII.1 Nuclear Data for Science and Technology: Cross Sections, Covariances, Fission Product Yields and Decay Data. *Nuclear Data Sheets*, 112:2887, 2011.

[4] D.A. Brown, M.B. Chadwick, R. Capote, A.C. Kahler, A. Trkov, M.W. Herman, A.A. Sonzogni, Y. Danon, A.D. Carlson, M. Dunn, D.L. Smith, G.M. Hale, G. Arbanas, R. Arcilla, C.R. Bates, B. Beck, B. Becker, F. Brown, R.J. Casperson, J. Conlin, D.E. Cullen, M.-A. Descalle, R. Firestone, T. Gaines, K.H. Guber, A.I. Hawari, J. Holmes, T.D. Johnson, T. Kawano, B.C. Kiedrowski, A.J. Koning, S. Kopecky, L. Leal, J.P. Lestone, C. Lubitz, J.I. Márquez Damián, C.M. Mattoon, E.A. McCutchan, S. Mughabghab, P. Navratil, D. Neudecker, G.P.A. Nobre, G. Noguere, M. Paris, M.T. Pigni, A.J. Plompen, B. Pritychenko, V.G. Pronyaev, D. Roubtsov, D. Rochman,

P. Romano, P. Schillebeeckx, S. Simakov, M. Sin, I. Sirakov, B. Sleaford, V. Sobes, E.S. Soukhovitskii, I. Stetcu, P. Talou, I. Thompson, S. van der Marck, L. Welser-Sherrill, D. Wiarda, M. White, J.L. Wormald, R.Q. Wright, M. Zerkle, G. Žerovnik, and Y. Zhu. ENDF/B-VIII.0: The 8^{th} Major Release of the Nuclear Reaction Data Library with CIELO-project Cross Sections, New Standards and Thermal Scattering Data. *Nuclear Data Sheets*, 148:1 – 142, 2018. ISSN 0090-3752. doi: https://doi.org/10.1016/j.nds.2018.02.001. URL https://www.sciencedirect.com/science/article/pii/S0090375218300206. Special Issue on Nuclear Reaction Data.

[5] John Bess et al. International Criticality Safety Benchmark Evaluation Project. URL http://icsbep.inel.gov.

[6] A.D. Carlson, V.G. Pronyaev, R. Capote, G.M. Hale, Z.-P. Chen, I. Duran, F.-J. Hambsch, S. Kunieda, W. Mannhart, B. Marcinkevicius, R.O. Nelson, D. Neudecker, G. Noguere, M. Paris, S.P. Simakov, P. Schillebeeckx, D.L. Smith, X. Tao, A. Trkov, A. Wallner, and W. Wang. Evaluation of the Neutron Data Standards. *Nuclear Data Sheets*, 148:143 – 188, 2018. ISSN 0090-3752. doi: https://doi.org/10.1016/j.nds.2018.02.002. URL http://www.sciencedirect.com/science/article/pii/S0090375218300218. Special Issue on Nuclear Reaction Data.

[7] M. Calviani, J. Praena, U. Abbondanno, G. Aerts, H. Álvarez, F. Álvarez-Velarde, S. Andriamonje, J. Andrzejewski, P. Assimakopoulos, L. Audouin, G. Badurek, P. Baumann, F. Bečvář, F. Belloni, B. Berthier, E. Berthoumieux, F. Calviño, D. Cano-Ott, R. Capote, C. Carrapiço, P. Cennini, V. Chepel, E. Chiaveri, N. Colonna, G. Cortes, A. Couture, J. Cox, M. Dahlfors, S. David, I. Dillmann, C. Domingo-Pardo, W. Dridi, I. Duran, C. Eleftheriadis, M. Embid-Segura, L. Ferrant, A. Ferrari, R. Ferreira-Marques, K. Fujii, W. Furman, I. Goncalves, E. González-Romero, A. Goverdovski, F. Gramegna, C. Guerrero, F. Gunsing, B. Haas, R. Haight, M. Heil, A. Herrera-Martinez, M. Igashira, E. Jericha,

F. Käppeler, Y. Kadi, D. Karadimos, D. Karamanis, V. Ketlerov, M. Kerveno, P. Koehler, V. Konovalov, E. Kossionides, M. Krtička, C. Lampoudis, H. Leeb, A. Lindote, I. Lopes, M. Lozano, S. Lukic, J. Marganiec, S. Marrone, T. Martínez, C. Massimi, P. Mastinu, A. Mengoni, P. M. Milazzo, C. Moreau, M. Mosconi, F. Neves, H. Oberhummer, S. O'Brien, J. Pancin, C. Papachristodoulou, C. Papadopoulos, C. Paradela, N. Patronis, A. Pavlik, P. Pavlopoulos, L. Perrot, M. T. Pigni, R. Plag, A. Plompen, A. Plukis, A. Poch, C. Pretel, J. Quesada, T. Rauscher, R. Reifarth, M. Rosetti, C. Rubbia, G. Rudolf, P. Rullhusen, J. Salgado, C. Santos, L. Sarchiapone, I. Savvidis, C. Stephan, G. Tagliente, J. L. Tain, L. Tassan-Got, L. Tavora, R. Terlizzi, G. Vannini, P. Vaz, A. Ventura, D. Villamarin, M. C. Vincente, V. Vlachoudis, R. Vlastou, F. Voss, S. Walter, M. Wiescher, and K. Wisshak. High-accuracy ^{233}U(n, f) cross-section measurement at the white-neutron source nTOF from near-thermal to 1 MeV neutron energy. *Phys. Rev. C*, 80:044604, Oct 2009. doi: 10.1103/PhysRevC.80.044604. URL https://link.aps.org/doi/10.1103/PhysRevC.80.044604.

[8] L. C. Leal, H. Derrien, J. A. Harvey, K. H. Guber, N. M. Larson, and R. R. Spencer. R-MATRIX RESONANCE ANALYSIS AND STATISTICAL PROPERTIES OF THE RESONANCE PARAMETERS OF ^{233}U IN THE NEUTRON ENERGY RANGE FROM THERMAL TO 600 EV. ORNL/TM report ORNL/TM-2000/372, Oak Ridge National Laboratory, 2001. Oak Ridge National Laboratory.

[9] K. H. Guber, R. R. Spencer, L. C. Leal, J. A. Harvey, N. W. Hill, G. Dos Santos, R. O. Sayer, and D. C. Larson. New High-Resolution Fission Cross-Section Measurements of 233U in the 0.4-eV to 700-keV Energy Range. *Nuclear Science and Engineering*, 135(2):141–149, 2000. doi: 10.13182/NSE00-A2130. URL https://doi.org/10.13182/NSE00-A2130.

[10] K. H. Guber, R. R. Spencer, L. C. Leal, P. E. Koehler, J. A. Harvey, R. O. Sayer, H. Derrien, T. E. Valentine, D. E. Pierce, V. M. Cauley, and

T. A. Lewis. High-Resolution Transmission Measurements of 233U Using a Cooled Sample at the Temperature T = 11 K. *Nuclear Science and Engineering*, 139(2):111–117, 2001. doi: 10.13182/NSE01-A2226. URL https://doi.org/10.13182/NSE01-A2226.

[11] Y. Peneliau, O. Litaize, P. Archier, and C. De Saint Jean. 239Pu Prompt Fission Neutron Spectra Impact on a Set of Criticality and Experimental Reactor Benchmarks. *Nuclear Data Sheets*, 118:459 – 462, 2014. ISSN 0090-3752. doi: https://doi.org/10.1016/j.nds.2014.04.106. URL http://www.sciencedirect.com/science/article/pii/S0090375214001367.

[12] R. Capote, Y.-J. Chen, F.-J. Hambsch, N.V. Kornilov, J.P. Lestone, O. Litaize, B. Morillon, D. Neudecker, S. Oberstedt, T. Ohsawa, N. Otuka, V.G. Pronyaev, A. Saxena, O. Serot, O.A. Shcherbakov, N.-C. Shu, D.L. Smith, P. Talou, A. Trkov, A.C. Tudora, R. Vogt, and A.S. Vorobyev. Prompt Fission Neutron Spectra of Actinides. *Nuclear Data Sheets*, 131:1 – 106, 2016. ISSN 0090-3752. doi: https://doi.org/10.1016/j.nds.2015.12.002. URL http://www.sciencedirect.com/science/article/pii/S0090375215000678. Special Issue on Nuclear Reaction Data.

[13] M. E. Rising, P. Talou, T. Kawano, and A. K. Prinja. Evaluation and Uncertainty Quantification of Prompt Fission Neutron Spectra of Uranium and Plutonium Isotopes. *Nuclear Science and Engineering*, 175(1):81–93, 2013. doi: 10.13182/NSE12-34. URL https://doi.org/10.13182/NSE12-34.

[14] IAEA Coordinated Research Project on Prompt Fission Neutron Spectra of actinides. URL https://www-nds.iaea.org/pfns/expdata/.

[15] Bacak, M., Aïche, M., Bélier, G., Berthoumieux, E., Diakaki, M., Dupont, E., Gunsing, F., Heyse, J., Kopecky, S., Krticka, M., Laurent, B., Leeb, H., Mathieu, L., Schillebeeckx, P., Serot, O., Taieb, J., Valenta, S., Vlachoudis, V., Aberle, O., Andrzejewski, J., Audouin, L., Balibrea, J., Barbagallo, M., Becvár, F., Billowes, J., Bosnar, D., Brown, A., Caamaño, M.,

Calviño, F., Calviani, Cano-Ott, D, Cardella, R., Casanovas, A., Cerutti, F., Chen, Y. H., Chiaveri, E., Colonna, Cortés, G., Cortés-Giraldo, M. A., Cosentino, L., Damone, L. A., Domingo-Pardo, C, Dressler, R., Durán, I., Fernández-Domínguez, B., Ferrari, A., Ferreira, P., Finocchiaro, P., Furman, V., Göbel, K., García, A. R., Gawlik, A., Gilardoni, S., Glodariu, T., Gonçalves, I. F., González-Romero, E., Griesmayer, E., Guerrero, C., Harada, H., Heinitz, S., Jenkins, D. G., Jericha, E., Käppeler, F., Kadi, Y., Kalamara, A., Kavrigin, P., Kimura, A., Kivel, N., Knapova, I., Kokkoris, M., Kurtulgil, D., Leal-Cidoncha, E, Lederer, C., Lerendegui-Marco, J, Meo, S. Lo, Lonsdale, S. J., Macina, D., Manna, A., Marganiec, J., Martínez, T., Masi, A., Massimi, C., Mastinu, P., Mastromarco, M., Maugeri, E. A., Mazzone, A., Mendoza, E., Mengoni, A., Milazzo, P. M., Mingrone, F., Musumarra, A., Negret, A., Nolte, R., Oprea, A., Patronis, N., Pavlik, A., Perkowski, J., Porras, I., Praena, J., Quesada, J. M., Radeck, D., Rauscher, T., Reifarth, R., Rubbia, C., Ryan, J. A., Sabaté-Gilarte, M., Saxena, A., Schumann, D., Sedyshev, P., Smith, A. G., Sosnin, N. V., Stamatopoulos, A., Tagliente, G., Tain, J. L., Tarifeño-Saldivia, A., Tassan-Got, L, Vannini, G., Variale, V., Vaz, P., Ventura, A., Vlastou, R., Wallner, A., Warren, S., Weiss, C., Woods, P. J., Wright, T., Zugec, P., and the n_TOF Collaboration. Preliminary results on the 233u io measurement at n_tof. *EPJ Web Conf.*, 239:01043, 2020. doi: 10.1051/epjconf/202023901043. URL https://doi.org/10.1051/epjconf/202023901043.

[16] P. Leconte, M. Antony, P. Archier, D. Bernard, C. De Saint Jean, J. Di Salvo, R. Eschbach, B. Geslot, A. Gruel, P. Tamagno, G. Truchet, and J.P. Hudelot. Validation of actinide nuclear data based on reactivity worth experiments in a mox-lwr spectrum. *Annals of Nuclear Energy*, 139: 107251, 2020. ISSN 0306-4549. doi: https://doi.org/10.1016/j.anucene.2019.107251. URL https://www.sciencedirect.com/science/article/pii/S0306454919307613.

[17] A. J. M. Plompen et al. The joint evaluated fission and fusion nuclear

data library, JEFF-3.3. *The European Physical Journal A*, 56:181, 2020. doi: 10.1140/epja/s10050-020-00141-9. URL https://doi.org/10.1140/epja/s10050-020-00141-9.

[18] W. P. Poenitz. Evaluation Methods for Neutron Cross Section Standards. Technical Report BNL-NCS-51363, Brookhaven National Laboratory, 1981. URL https://www-nds.iaea.org/standards/codes.html.

[19] V. G. Pronyaev B. Marcinkevicius, S. Simakov. Short User Guide of Generalized Least Squares Code GMAP. URL https://www-nds.iaea.org/standards/Codes/GMA-User-Guide.pdf.

[20] W. Mannhart. Evaluation of the Cf-252 Fission Neutron Spectrum between 0 MeV and 20 MeV. Technical Report IAEA-TECDOC-410, International Atomic Energy Agency, 1987.

[21] W. Mannhart. Status of the Cf-252 Fission Neutron Spectrum Evaluation with Regard to Recent Experiments. Technical Report INDC(NDS)-220, International Atomic Energy Agency, 1988.

[22] A. Trkov, P.J. Griffin, S.P. Simakov, L.R. Greenwood, K.I. Zolotarev, R. Capote, D.L. Aldama, V. Chechev, C. Destouches, A.C. Kahler, C. Konno, M. Kotl, M. Majerle, E. Malambu, M. Ohta, V.G. Pronyaev, V. Radulovi, S. Sato, M. Schulc, E. imekov, I. Vavtar, J. Wagemans, M. White, and H. Yashima. IRDFF-II: A New Neutron Metrology Library. *Nuclear Data Sheets*, 163:1 – 108, 2020. ISSN 0090-3752. doi: https://doi.org/10.1016/j.nds.2019.12.001. URL http://www.sciencedirect.com/science/article/pii/S0090375219300687.

[23] Capote, R., Smith, D.L., and Trkov, A. Nuclear data evaluation methodology including estimates of covariances. *EPJ Web of Conferences*, 8:04001, 2010. doi: 10.1051/epjconf/20100804001. URL https://doi.org/10.1051/epjconf/20100804001.

[24] R. Capote D. L. Smith, D. Neudecker. Prompt Fission Neutron Spectrum Evaluation Techniques. Technical Report INDC(NDS)-0678, International Atomic Energy Agency, 2015.

[25] M.B. Chadwick, P. Obloinsk, M. Herman, N.M. Greene, R.D. McKnight, D.L. Smith, P.G. Young, R.E. MacFarlane, G.M. Hale, S.C. Frankle, A.C. Kahler, T. Kawano, R.C. Little, D.G. Madland, P. Moller, R.D. Mosteller, P.R. Page, P. Talou, H. Trellue, M.C. White, W.B. Wilson, R. Arcilla, C.L. Dunford, S.F. Mughabghab, B. Pritychenko, D. Rochman, A.A. Sonzogni, C.R. Lubitz, T.H. Trumbull, J.P. Weinman, D.A. Brown, D.E. Cullen, D.P. Heinrichs, D.P. McNabb, H. Derrien, M.E. Dunn, N.M. Larson, L.C. Leal, A.D. Carlson, R.C. Block, J.B. Briggs, E.T. Cheng, H.C. Huria, M.L. Zerkle, K.S. Kozier, A. Courcelle, V. Pronyaev, and S.C. van der Marck. ENDF/B-VII.0: Next Generation Evaluated Nuclear Data Library for Nuclear Science and Technology. *Nuclear Data Sheets*, 107(12): 2931 – 3060, 2006. ISSN 0090-3752. doi: https://doi.org/10.1016/j.nds.2006.11.001. URL http://www.sciencedirect.com/science/article/pii/S0090375206000871. Evaluated Nuclear Data File ENDF/B-VII.0.

[26] A. Trkov, R. Capote, and V.G. Pronyaev. Current Issues in Nuclear Data Evaluation Methodology: 235U Prompt Fission Neutron Spectra and Multiplicity for Thermal Neutrons. *Nuclear Data Sheets*, 123:8 – 15, 2015. ISSN 0090-3752. doi: https://doi.org/10.1016/j.nds.2014.12.003. URL http://www.sciencedirect.com/science/article/pii/S0090375214006826. Special Issue on International Workshop on Nuclear Data Covariances April 28 - May 1, 2014, Santa Fe, New Mexico, USA http://t2.lanl.gov/cw2014.

[27] A. Trkov and R. Capote. Evaluation of the Prompt Fission Neutron Spectrum of Thermal-neutron Induced Fission in U-235. *Physics Procedia*, 64: 48 – 54, 2015. ISSN 1875-3892. doi: https://doi.org/10.1016/j.phpro.2015.04.007. URL http://www.sciencedirect.com/science/article/

pii/S1875389215001236. Scientific Workshop on Nuclear Fission Dynamics and the Emission of Prompt Neutrons and Gamma Rays, THEORY-3.

[28] OECD, Nuclear Energy Agency, Collaborative International Evaluated Library Organisation (CIELO) Pilot Project, WPEC Subgroup 40 (SG40). URL https://www.oecd-nea.org/science/wpec/sg40-cielo/.

[29] IAEA CIELO Data Development Project within the International Pilot Project of the OECD/NEA [28], 2014. URL https://www-nds.iaea.org/CIELO/.

[30] M.B. Chadwick, E. Dupont, E. Bauge, A. Blokhin, O. Bouland, D.A. Brown, R. Capote, A. Carlson, Y. Danon, C. De Saint Jean, M. Dunn, U. Fischer, R.A. Forrest, S.C. Frankle, T. Fukahori, Z. Ge, S.M. Grimes, G.M. Hale, M. Herman, A. Ignatyuk, M. Ishikawa, N. Iwamoto, O. Iwamoto, M. Jandel, R. Jacqmin, T. Kawano, S. Kunieda, A. Kahler, B. Kiedrowski, I. Kodeli, A.J. Koning, L. Leal, Y.O. Lee, J.P. Lestone, C. Lubitz, M. MacInnes, D. McNabb, R. McKnight, M. Moxon, S. Mughabghab, G. Noguere, G. Palmiotti, A. Plompen, B. Pritychenko, V. Pronyaev, D. Rochman, P. Romain, D. Roubtsov, P. Schillebeeckx, M. Salvatores, S. Simakov, E.Sh. Soukhovitski, J.C. Sublet, P. Talou, I. Thompson, A. Trkov, R. Vogt, and S. van der Marck. The CIELO Collaboration: Neutron Reactions on 1H, 16O, 56Fe, 235,238U, and 239Pu. *Nuclear Data Sheets*, 118:1 – 25, 2014. ISSN 0090-3752. doi: https://doi.org/10.1016/j.nds.2014.04.002. URL http://www.sciencedirect.com/science/article/pii/S0090375214000325.

[31] M.B. Chadwick, R. Capote, A. Trkov, M.W. Herman, D.A. Brown, G.M. Hale, A.C. Kahler, P. Talou, A.J. Plompen, P. Schillebeeckx, M.T. Pigni, L. Leal, Y. Danon, A.D. Carlson, P. Romain, B. Morillon, E. Bauge, F.-J. Hambsch, S. Kopecky, G. Giorginis, T. Kawano, J. Lestone, D. Neudecker, M. Rising, M. Paris, G.P.A. Nobre, R. Arcilla, O. Cabellos, I. Hill, E. Dupont, A.J. Koning, D. Cano-Ott, E. Mendoza, J. Balibrea, C. Pa-

radela, I. Durn, J. Qian, Z. Ge, T. Liu, L. Hanlin, X. Ruan, W. Haicheng, M. Sin, G. Noguere, D. Bernard, R. Jacqmin, O. Bouland, C. De Saint Jean, V.G. Pronyaev, A.V. Ignatyuk, K. Yokoyama, M. Ishikawa, T. Fukahori, N. Iwamoto, O. Iwamoto, S. Kunieda, C.R. Lubitz, M. Salvatores, G. Palmiotti, I. Kodeli, B. Kiedrowski, D. Roubtsov, I. Thompson, S. Quaglioni, H.I. Kim, Y.O. Lee, U. Fischer, S. Simakov, M. Dunn, K. Guber, J.I. Mrquez Damin, F. Cantargi, I. Sirakov, N. Otuka, A. Daskalakis, B.J. McDermott, and S.C. van der Marck. CIELO Collaboration Summary Results: International Evaluations of Neutron Reactions on Uranium, Plutonium, Iron, Oxygen and Hydrogen. *Nuclear Data Sheets*, 148: 189 – 213, 2018. ISSN 0090-3752. doi: https://doi.org/10.1016/j.nds.2018.02.003. URL http://www.sciencedirect.com/science/article/pii/S009037521830022X. Special Issue on Nuclear Reaction Data.

[32] R. Capote, A. Trkov, M. Sin, M.T. Pigni, V.G. Pronyaev, J. Balibrea, D. Bernard, D. Cano-Ott, Y. Danon, A. Daskalakis, T. Gorianec, M.W. Herman, B. Kiedrowski, S. Kopecky, E. Mendoza, D. Neudecker, L. Leal, G. Noguere, P. Schillebeeckx, I. Sirakov, E.S. Soukhovitskii, I. Stetcu, and P. Talou. IAEA CIELO Evaluation of Neutron-induced Reactions on 235U and 238U Targets. *Nuclear Data Sheets*, 148:254 – 292, 2018. ISSN 0090-3752. doi: https://doi.org/10.1016/j.nds.2018.02.005. URL http://www.sciencedirect.com/science/article/pii/S0090375218300243. Special Issue on Nuclear Reaction Data.

[33] R. E. Kalman. A New Approach to Linear Filtering and Prediction Problems. *Journal of Basic Engineering*, 82(1):35–45, 03 1960. ISSN 0021-9223. doi: 10.1115/1.3662552. URL https://doi.org/10.1115/1.3662552.

[34] David G. Madland and J. Rayford Nix. New Calculation of Prompt Fission Neutron Spectra and Average Prompt Neutron Multiplicities. *Nuclear Science and Engineering*, 81(2):213–271, 1982. doi: 10.13182/NSE82-5. URL https://doi.org/10.13182/NSE82-5.

[35] L. W. Weston, R. Gwin, G. deSaussure, R. R. Fullwood, and R. W. Hockenbury. Measurement of the Neutron Fission and Capture Cross Sections for 233U in the Energy Region 0.4 to 2000 eV. *Nuclear Science and Engineering*, 34(1):1–12, 1968. doi: 10.13182/NSE68-A19361. URL https://doi.org/10.13182/NSE68-A19361.

[36] L. W. Weston, R. Gwin, G. de Saussure, R. W. Ingle, J. H. Todd, C.W. Craven, R. W. Hockenbury, and R. C. Block. Neutron Fission and Capture Cross-Section Measurements for Uranium-233 in the Energy Region 0.02 to 1 eV. *Nuclear Science and Engineering*, 42(2):143–149, 1970. doi: 10.13182/NSE70-A19495. URL https://doi.org/10.13182/NSE70-A19495.

[37] M. S. Moore, L. G. Miller, and O. D. Simpson. Slow Neutron Total and Fission Cross Sections of U^{233}. *Phys. Rev.*, 118:714–717, May 1960. doi: 10.1103/PhysRev.118.714. URL https://link.aps.org/doi/10.1103/PhysRev.118.714.

[38] N. J. Pattenden and J. A. Harvey. Measurement of the Neutron Total Cross Section of U233 from 0.07 to 10,000 eV. *Nuclear Science and Engineering*, 17(3):404–410, 1963. doi: 10.13182/NSE63-A17389. URL https://doi.org/10.13182/NSE63-A17389.